Title

ROS-mediated SRMS activation confers platinum resistance in ovarian cancer.

Journal

Oncogene, 42(20)

Authors

Jiang, Yunhan
Song, Lina
Lin, Yizhu
et al.

Publication Date

2023-05-01

DOI

10.1038/s41388-023-02679-6

Peer reviewed

HHS Public Access

Author manuscript

Oncogene. Author manuscript; available in PMC 2023 November 01.

Published in final edited form as:

Oncogene. 2023 May ; 42(20): 1672–1684. doi:10.1038/s41388-023-02679-6.

ROS-mediated SRMS activation confers platinum resistance in ovarian cancer

Yunhan Jiang[1], **Lina Song**[1], **Yizhu Lin**[2], **Pawel Nowialis**[1], **Qiongmei Gao**[1], **Tao Li**[3], **Bin Li**[3], **Xiaobo Mao**[4], **Qianqian Song**[5], **Chengguo Xing**[6], **Guangrong Zheng**[6], **Shuang Huang**[3], **Lingtao Jin**[1,*]

[1]Department of Molecular Medicine, Long School of Medicine, University of Texas Health Science Center at San Antonio, San Antonio, TX 78229

[2]Department of Cell and Tissue Biology, School of Dentistry, University of California San Francisco, San Francisco, CA 94143

[3]Department of Anatomy and Cell Biology, College of Medicine, University of Florida, Gainesville, FL 32610

[4]Institute for Cell Engineering, Department of Neurology, Johns Hopkins University School of Medicine, Baltimore, MD 21205

[5]Department of Cancer Biology, Wake Forest School of Medicine, Winston-Salem, NC 27101

[6]Department of Medicinal Chemistry, College of Pharmacy, University of Florida, Gainesville, FL 32610

Abstract

Ovarian cancer is the leading cause of death among gynecological malignancies. Checkpoint blockade immunotherapy has so far only shown modest efficacy in ovarian cancer and platinum-based chemotherapy remains the front-line treatment. Development of platinum resistance is one of the most important factors contributing to ovarian cancer recurrence and mortality. Through kinome-wide synthetic lethal RNAi screening combined with unbiased datamining of cell line platinum response in CCLE and GDSC databases, here we report that Src-Related Kinase Lacking C-Terminal Regulatory Tyrosine And N-Terminal Myristylation Sites (SRMS), a non-receptor tyrosine kinase, is a novel negative regulator of MKK4-JNK signaling under platinum treatment and plays an important role in dictating platinum efficacy in ovarian cancer. Suppressing SRMS specifically sensitizes p53-deficient ovarian cancer cells to platinum *in vitro* and *in vivo*. Mechanistically, SRMS serves as a “sensor” for platinum-induced ROS. Platinum treatment-induced ROS activates SRMS, which inhibits MKK4 kinase activity by directly phosphorylating MKK4 at Y269 and Y307, and consequently attenuates MKK4-JNK activation.

[*]Correspondence: jinl1@uthscsa.edu ; Lingtao Jin, University of Texas Health Science Center at San Antonio, San Antonio, TX; Tel.: 210-450-7264.

AUTHOR CONTRIBUTIONS

L.J. and Y.J. conceived and designed this study. Y.J. performed all experiments with assistance from L.S., P.N., Q.G., T.L. and L.J.. B.L. provided critical reagents. Y.L. performed analysis of RNA-sequencing data. X.M., Q.S., C.X., G.Z. and S.H. provided experimental advices. L.J. and Y.J. wrote the paper. L.J. supervised the project.

COMPETING INTERESTS

The authors declare no competing interests.

Suppressing SRMS leads to enhanced MKK4-JNK-mediated apoptosis by inhibiting MCL1 transcription, thereby boosting platinum efficacy. Importantly, through a “drug repurposing” strategy, we uncovered that PLX4720, a small molecular selective inhibitor of B-RafV^{600E}, is a novel SRMS inhibitor that can potently boost platinum efficacy in ovarian cancer *in vitro* and *in vivo*. Therefore, targeting SRMS with PLX4720 holds the promise to improve the efficacy of platinum-based chemotherapy and overcome chemoresistance in ovarian cancer.

Keywords

Platinum-based chemotherapy; platinum resistance; SRMS; JNK; PLX4720

INTRODUCTION

Ovarian cancer remains the most lethal gynecologic cancer(1). Platinum-based standard of care in ovarian cancer (e.g. cisplatin or carboplatin plus taxane) usually leads to robust initial clinical response but patients eventually succumb to chemoresistant recurrence(1). In addition, checkpoint blockade immunotherapy has only shown modest efficacy in ovarian cancer(2-4). Over the decades, extensive efforts have been made to identify key molecules and events critical for platinum resistance in ovarian cancer. However, strategies developed thus far have only achieved limited success(5). The anti-tumor activity of platinum is mediated mainly through forming persistent DNA interstrand crosslinks (ICLs), leading to DNA damage and apoptosis(6, 7). In addition to DNA, platinum can interact with a wide number of cytoplasmic substrates such as reduced glutathione, methionine, and proteins, all of which can also contribute to platinum’s antitumor effect(8, 9). Despite extensive studies, the mechanism of platinum resistance in ovarian cancer is still not fully understood, partly due to the complex nature of resistance mechanisms. Several potential mechanisms for platinum resistance have been proposed including changes in drug efflux/breakdown, increased repair of DNA damage, increased activation of pro-survival pathways or inhibition of cell apoptosis pathways, among others(6, 7). Given the extensive use of platinum-based therapy in ovarian cancer patients, identification of druggable pathways that regulate the cellular response to platinum holds the key to improve platinum efficacy and overcome resistance.

Given the fact that protein kinases play important roles in the regulation of pro-survival signaling(10-13), we previously employed a kinome-wide shRNA screening and identified microtubule-associated serine/threonine kinase 1 (MAST1) as a “synthetic lethal” partner of cisplatin in head and neck cancer(14). In our attempt to develop a therapeutic strategy to improve platinum-based therapy in ovarian cancer, we utilized this strategy and identified Src-Related Kinase Lacking C-Terminal Regulatory Tyrosine And N-Terminal Myristylation Sites (SRMS), a nonreceptor tyrosine kinase that belongs to the Brk family(15), as a critical player in mediating platinum resistance, particularly in p53-deficient ovarian cancer. In this study, we uncover that SRMS serves as a “sensor” for platinum-induced reactive oxygen species (ROS). Platinum-induced ROS activates SRMS, which reduces platinum efficacy by negatively regulating mitogen-activated protein kinase kinase 4 (MKK4) kinase activity and c-Jun N-terminal kinase family (JNK) signaling. Inhibition of MKK4-JNK signaling

by SRMS leads to reduced apoptosis in ovarian cancer cells. Through a drug repurposing strategy, we further identify B-Raf^{V600E} inhibitor PLX4720 as a potent SRMS inhibitor that can be used to boost the efficacy of platinum in ovarian cancer. This study suggests SRMS may be a promising target to improve the platinum-based chemotherapy for ovarian cancer patients.

RESULTS

SRMS expression is associated with platinum resistance in ovarian cancer.

As part of our larger effort to identify kinases that are required for resistance to cisplatin or paclitaxel, two of the most widely used chemotherapy agents, we previously performed a kinome-wide synthetic lethal RNAi screening using a lentiviral shRNA library targeting 781 human kinase and kinase-related genes (4,518 clones)(14). We identified protein kinase MAST1 as a synthetic lethal partner of cisplatin in head and neck cancer(14). To search for additional candidates that maybe critical for conferring platinum resistance in other cancer types where platinum currently serves as front-line treatment, we performed correlation analysis on gene expressions of the top 50 candidates from our primary screening(14) vs platinum sensitivity in a variety of cancer types using two drug sensitivity cell line databases, CCLE(16) and GDSC(17). These unbiased analyses revealed that expressions of SRMS and Macrophage Stimulating 1 Receptor (MST1R) are strongly correlated with cisplatin or carboplatin resistance in ovarian cancer cell lines from both datasets (Figures 1A-1B). Because MST1R had been linked to cisplatin resistance in ovarian cancer in a previous publication (18), we sought to explore whether SRMS plays a role in regulating platinum sensitivity in ovarian cancer. To confirm the initial correlation analysis, we assembled a panel of human ovarian cancer cell lines and determined their SRMS gene expression levels and platinum sensitivity. Indeed, we were able to confirm the positive correlation between SRMS level and platinum resistance (Figure 1C). Furthermore, we developed platinum-resistant ovarian cancer cell lines (OVCAR4 and ES-2) using an escalating dose of platinum (Figures S1A-S1B). Interestingly, SRMS levels were elevated in these platinum-resistant sublines, compared to their parental lines (Figure 1D). We also performed immunohistochemical staining using primary tissue microarray samples from ovarian cancer patients and found that SRMS levels were correlated with progressive stages of ovarian cancer in patients (Figure 1E). To further investigate the relevance of SRMS to platinum resistance, we analyzed the association between SRMS expression and patient survival using publicly available databases(19). The analysis of platinum-treated ovarian cancer patients revealed that high SRMS expression was correlated with not only worse overall survival but also lower progression-free survival (Figures 1F-1G). The inverse correlation between SRMS expression and progression-free survival strongly suggests that ovarian cancer patients with high SRMS expression may respond poorly to platinum-based chemotherapy.

Silencing SRMS boosts platinum efficacy in ovarian cancer

To delineate the functional role of SRMS in ovarian cancer, we generated SRMS stable knockdown ES-2 cells using two sequence-distinct SRMS shRNAs (Figure S1A). Cell viability assays showed that silencing SRMS did not significantly affect cell viability, but

markedly sensitized cells to platinum (Figure 2A, Figure S1C). Silencing SRMS in ES-2 cisplatin-resistant subline also sensitized them to platinum treatment (Figure 2B, Figure S1D). We subsequently analyzed the IC_{50} of platinum in a panel of ovarian cancer cell lines expressing control vector or SRMS shRNA. We found that knockdown of SRMS effectively reduced IC_{50} of platinum in all p53-deficient lines (OVCAR3, ES-2, SKOV3, OVCAR8, OVCAR4, CAOV3) but only slightly altered IC_{50} of platinum in p53-competent lines (TOV21G, HEY) (Figure 2C). Colony formation and cell counting assays further demonstrated that silencing SRMS significantly attenuated cell viability in the presence of platinum, but only marginally impacted cell viability in the absence of platinum (Figures 2D-2E). Xenograft assays using intraperitoneal model confirmed that silencing SRMS sensitized both ES-2 parental line and platinum-resistant subline to platinum *in vivo* (Figures 2F-2G, Figure S2). Immunohistochemistry analysis of tumors showed that SRMS silencing enhanced platinum-induced apoptosis in tumors (Figure 2H). These results demonstrate that SRMS plays an important role in regulating the platinum response in ovarian cancer cells, particularly in p53-deficient ovarian cancer such as high-grade serous carcinoma that accounts for three quarters of ovarian carcinoma and frequently shows p53 inactivation(5, 20).

Platinum compounds including cisplatin and carboplatin induce DNA damage in cancer cells, causing cell cycle arrest and apoptosis(6, 7). To investigate the underlying mechanism by which SRMS knockdown sensitizes cells to platinum, we first examined whether silencing SRMS increases platinum-induced DNA damage. As shown in Figure 3A, platinum treatment robustly induced p-γH2AX, the marker of DNA damage. Interestingly, SRMS silencing did not further increased platinum-induced DNA damage, but strongly boosted apoptosis, as measured by p-γH2AX and cleaved-PARP (c-PARP) levels (Figure 3A), suggesting SRMS knockdown promoted platinum-induced apoptosis through a DNA damage-independent mechanism. We also performed single-cell gel electrophoresis (comet assay) to examine platinum-induced DNA damage in vector control or SRMS knockdown cells. Consistent with the data from p-γH2AX staining, comet assay also demonstrated that platinum-induced DNA damage is comparable between vector control and SRMS knockdown cells (Figure S3A). 7-AAD staining showed that SRMS silencing did not significantly affect platinum-induced cell cycle arrest (Figure 3B). Platinum compounds such as cisplatin have been shown to react with and deplete intracellular glutathione (GSH), leading to oxidative stress(8, 21, 22). Indeed, platinum-induced ROS can contribute to DNA damage and cell death. However, neither ROS nor GSH levels were affected by SRMS silencing (Figures S3B-S3C), suggesting SRMS is unlikely to play a role in regulating platinum-induced oxidative stress. To further investigate whether SRMS plays any role in regulating cell cycle progression under platinum treatment, we synchronized ES-2 cells expressing control vector or SRMS shRNA using double hydroxyurea (HU) block, followed by release and platinum treatment (Figure S3D). We then collected cells at different time points and examined the cell cycle progression, DNA damage and apoptosis simultaneously. We found that silencing SRMS did not impact platinum-induced cell cycle arrest or DNA damage, but still increased apoptosis (Figure S3D), further demonstrating a potential regulatory role of SRMS in platinum-induced apoptosis. We therefore hypothesized that SRMS silencing directly enhanced platinum-induced apoptosis. Indeed, annexin V/PI

staining, caspase activity and cytochrome c release assays all demonstrated that silencing of SRMS led to enhanced platinum-induced apoptosis (Figures 3C-3E). Consistently, RNA sequencing with Gene Set Enrichment Analysis (GSEA) revealed that SRMS knockdown cells were enriched for apoptosis signature genes (Figure 3F). We then analyzed other DNA damaging agents with diverse modes of action as well as the anti-tubulin agent paclitaxel in ovrian cancer cells and found that the pro-apoptotic effect of SRMS knockdown was specific to platinum (Figures 3G-3H, Figure S3E). These data collectively suggest that SRMS may reduce the efficacy of platinum by inhibiting platinum-induced apoptosis.

Platinum-induced reactive oxygen species activates SRMS

We initially observed that platinum treatment promoted SRMS autophosphorylation and SRMS kinase activity (Figures 4A-4C). We therefore sought to investigate how SRMS is activated by platinum. It has been well-documented that platinum compounds can disrupt cellular glutathione homeostasis that leads to elevated reactive oxygen species (ROS) level and oxidative stress(8, 22-24). Given that intracellular ROS has been shown to activate certain kinases(25-27), we therefore explored whether platinum-induced ROS could activate SRMS. Indeed, similar with platinum, H_2O_2 treatment strongly increased SRMS autophosphorylation and boosted SRMS kinase activity in ES-2 cells (Figures 4D-4F). An *in vitro* SRMS kinase assay further demonstrated that H_2O_2 directly promoted SRMS activity (Figure 4G). Importantly, ROS scavenger Trolox significantly reduced platinum-induced ROS and blunted the increase of SRMS autophosphorylation and kinase activity induced by platinum treatment (Figures 4H-4J). Collectively, these data suggest that SRMS can serve as an ROS sensor in response to platinum treatment, and that platinum-induced ROS can directly activate SRMS activity in ovarian cancer cells.

SRMS ameliorates platinum-induced JNK activation

Given that SRMS kinase activity is upregulated by platinum, we hypothesized that SRMS may inhibit platinum-induced apoptosis by phosphorylating key downstream signaling effectors involved in the apoptosis pathway. We performed a phospho-kinase array analysis and identified a dramatic increase in c-Jun Ser63 phosphorylation (Ser63) in platinum-treated SRMS knockdown cells, compared to vector control (Figure 4K), suggesting SRMS may be an upstream negative regulator of c-Jun signaling. Ser63 of c-Jun is a well-known JNK phosphorylation site. Importantly, the MKK-JNK-c-Jun axis plays a central role in cellular stress signaling, by sensing a variety of stress factors, such as cytokines, growth factors, oxidative stress, and chemotherapy agents. The prolonged activation of the MKK-JNK-c-Jun pathway leads to induction of apoptosis(28-32). Indeed, we found that platinum treatment led to strong activation of JNK-c-Jun signaling and apoptosis in parental ES-2 cells, but not in platinum resistant line (Figure 4L). Therefore, we reasoned that SRMS may prevent platinum-induced MKK-JNK-c-Jun activation, leading to reduced apoptosis. Indeed, platinum induced much greater increase in p-c-Jun level in SRMS-knockdown than those in control cells (Figure 4M). The phosphorylation of JNK and MKK4, the upstream kinase cascade for cJun signaling, were also increased in SRMS-knockdown when treated with platinum, suggesting the MKK4-JNK-cJun axis is hyper-activated in SRMS-knockdown cells in response to platinum (Figure 4M). We did not observe this hyper-activation in ERK and p38 signaling (Figure 4M). Importantly, these results are consistent with our initial

shRNA screening in which JNK1 was identified as a top hit whose knockdown made cells more resistant to cisplatin treatment(14). Also, silencing JNK2 or MKK4, or treatment with JNK inhibitor, all reduced platinum-induced apoptosis in multiple ovarian cancer cell lines (Figure 4N, Figure S4A), confirming an important role of MKK-JNK signaling in mediating platinum effect. Importantly, silencing MKK4 using shRNA partially rescued the enhanced apoptosis induced by platinum in SRMS knockdown cells (Figure 4O). In addition, JNK inhibitor, but not ERK or p38 inhibitor, significantly reduced the platinum-induced apoptosis in SRMS knockdown cells (Figure 4P). In ovarian cancer patient samples, we also observed that SRMS levels inversely correlated with p-c-Jun levels (Figures 4Q-4R). These results collectively suggest that SRMS blocks MKK4-JNK-cJun signaling in response to platinum in ovarian cancer cells. Inhibition of SRMS leads to hyper-activation of MKK4-JNK-cJun signaling and consequently enhanced apoptosis.

SRMS directly phosphorylates and inhibits MKK4 kinase activity

Given that SRMS is a kinase, and that silencing SRMS increased the phosphorylation of both JNK and its upstream kinase MKK4, we hypothesized that SRMS may directly bind to and phosphorylate MKK4 to inhibit MKK4-JNK-cJun signaling. Indeed, both immunoprecipitation and bimolecular fluorescence complementation (BiFC) assays(33) demonstrated that SRMS directly interacts with MKK4 in the cell (Figures 5A-5C). Further an SRMS *in vitro* kinase assay demonstrated that SRMS directly phosphorylates MKK4 *in vitro* (Figure 5D). To determine whether SRMS is sufficient to inhibit MKK4 kinase activity directly, we performed a two-stage SRMS and MKK4 kinase activity assay using inactive JNK1 as a substrate and found that SRMS-mediated MKK4 phosphorylation directly inhibits MKK4 kinase activity (Figure 5E).

To provide further mechanistic insight into how SRMS inhibits MKK4 activity, we performed mass spectrometry analysis and identified MKK4 Y269 and MKK4 Y307 as potential phosphorylation sites by SRMS (Figures 5F-5G). To investigate how Y269 and Y307 phosphorylation regulates MKK4 activity, we generated MKK4 Y269F and Y307F phosphor-deficient mutants. The two-stage SRMS and MKK4 kinase activity assay showed that Y269F or Y307F mutations significantly attenuated SRMS-mediated MKK4 inhibition (Figure 5H). Furthermore, compared to wild-type MKK4, expressing Y269F or Y307F mutants led to increased MKK4 activity in the presence of platinum (Figure 5I), as measured by JNK phosphorylation, suggesting Y269 and Y307 serve as inhibitory phosphorylation sites for MKK4. Overall, our data suggests a model in which SRMS inhibits MKK4 activity via phosphorylation of MKK4 at Y269 and Y307 to limit platinum-induced MKK-JNK-cJun signaling activation (Figure 5J).

SRMS-MKK4-JNK signaling promotes MCL1 expression to counter platinum-induced apoptosis

MKK-JNK signaling plays an important role in mediating cellular stress responses such as apoptosis(28-30). For example, JNK has been shown to promote apoptosis through c-Jun-dependent transcription regulation by regulating the expression of Bcl-2 family members such as NOXA, BIM, and MCL1(29, 32, 34). JNK can also regulate apoptosis through c-Jun-independent mechanisms by directly phosphorylating Bcl-2 family members including

MCL1 and BMF (28, 29, 34). To obtain further insight regarding how SRMS-MKK-JNK modulates platinum-induced apoptosis in ovarian cancer cells, we profiled the expressions of Bcl-2 family members by qRT-PCR and western blotting. We found that both protein and mRNA levels of the anti-apoptotic protein MCL1 were significantly reduced in SRMS knockdown cells, compared to vector control cells (Figures 6A-6C). This phenomenon is particularly obvious after platinum treatment. No significant differences were found for other Bcl-2 family members. Importantly, ectopic expression of MCL1 rescued enhanced apoptosis in SRMS knockdown cells (Figure 6D), demonstrating an important role for MCL1 in mediating the effect of SRMS.

Because MCL1 levels are regulated at both the transcriptional and post-translational levels(35-37), and JNK has been shown to directly phosphorylate MCL1 and weaken its stability in certain cancers(32, 34), we sought to determine whether the reduced MCL1 level observed in SRMS knockdown ovarian cancer cells were due to enhanced protein degradation. However, cycloheximide chasing assay showed that MCL1 stability was not decreased in SRMS knockdown cells (Figure S5A). Proteasome inhibitor MG-132 also failed to rescue the reduced MCL1 level in SRMS knockdown cells (Figure S5B). Actinomycin D chasing assay also showed that compared with vector control cells, MCL1 mRNA stability was not decreased but rather slightly increased in SRMS knockdown cells when treated with cisplatin (Figure S5C). These data suggest that SRMS-JNK may regulate MCL1 levels through repressing MCL1 gene expression.

In support of this hypothesis, we observed that MCL1 promoter activity was greatly reduced in SRMS knockdown cells (Figure 6E), which could be rescued by the JNK inhibitor (Figure 6F). Given the critical role of c-Jun in mediating JNK's effects on gene expression regulation, we further performed p-c-Jun Cleavage Under Targets and Release Using Nuclease assay (CUT&RUN)(38, 39) to examine whether c-Jun is directly recruited to the MCL1 promoter. Indeed, SRMS silencing led to enhancement of p-c-Jun binding to the MCL1 promoter, which could be blunted by the JNK inhibitor (Figure 6G). Collectively, our data support a model in which SRMS inhibits MKK4 activation in response to platinum in ovarian cancer cells. Silencing SRMS promotes activation of MKK4-JNK-c-Jun in response to platinum, resulting in repression of MCL1 expression and enhanced apoptosis (Figure 6H). It is conceivable that upon SRMS inhibition, c-Jun may recruit certain transcriptional suppressors to MCL1 promoter to reduce MCL1 gene expression. The detailed mechanism by which SRMS regulates MCL1 gene expression certainly warrants further investigation.

Identification of PLX4720 as novel SRMS inhibitor to boost platinum-based therapy

Our data that silencing SRMS sensitized ovarian cancer cells to platinum suggest the potential to therapeutically target SRMS to enhance platinum-based chemotherapy in HGSOC. In our attempt to target SRMS pharmacologically, we searched IUPHAR database which provides binding reactivity of 72 inhibitors against 456 kinases (Figure 7A, (40)) and found 10 inhibitors that are capable of binding to SRMS. We subsequently performed *in vitro* SRMS kinase assay and found that PLX4720, a B-RAF^{V600E} inhibitor(41), was the most effective in inhibiting SRMS activity (Figure 7B). Consistently, previous studies have also found that PLX4720 and its related B-RAF^{V600E} inhibitors potently inhibit SRMS

kinase activity *in vitro*(42, 43). We therefore sought to test whether PLX4720 can sensitize ovarian cancer cells to platinum treatment. Indeed, PLX4720 treatment significantly reduced cisplatin IC_{50} in ovarian cancer cells (Figure 7C). An ATP competition assay showed that PLX4720 inhibited SRMS by competing with ATP (Figure 7D). In addition, western blotting confirmed that PLX4720 dose-dependently inhibited SRMS autophosphorylation (Figure 7E). We subsequently examined whether PLX4720 enhances platinum-induced MKK4-JNK activation, and consequently reduces MCL1 level. Similar with the SRMS knockdown cells, PLX4720 and cisplatin combination showed increased MKK4 and JNK phosphorylation in ovarian cancer cell lines, compared with cisplatin alone (Figure 7F). In addition, PLX4720 and cisplatin combination led to reduced MCL1 level and increased PARP cleavage (Figure 7F). Based on these observations, we evaluated whether PLX4720 can boost platinum efficacy in ovarian cancer cells *in vivo*. As previously reported, PLX4720 is well-tolerated *in vivo*(41). Strikingly, combined treatment of PLX4720 with cisplatin led to reduced tumor growth, increased level of phospho-c-Jun, and caspase 3 activation in ES-2 xenograft mice (Figures 7G-7I). Similar results were also obtained in ES-2 cisplatin resistant subline (Figure S6). These results identify PLX4720 as a potential therapeutic agent to suppress SRMS activity and boost platinum efficacy in ovarian cancer.

DISCUSSION

Here, we uncover SRMS as an important regulator of platinum sensitivity in ovarian cancer. Although the physiological substrates of SRMS remain largely unknown(44), several recent studies have provided insight into the cellular function of SRMS. For example, a previous proteomic study identified DOK1, Vimentin and Sam68 as bona fide SRMS substrates(45). Interestingly, a recent study has demonstrated that under nutrient-rich conditions, SRMS inhibits autophagy and promotes breast cancer growth by phosphorylating the scaffolding protein FKBP51(15), demonstrating a role for SRMS in regulating the cellular response to environmental cues. In this current study, we found that SRMS plays an important role in modulating MKK-JNK activation in response to platinum treatment. The stress-activated c-Jun NH2-terminal kinase (JNK) pathway belongs to the family of MAP-kinases involved in the regulation of cell proliferation, differentiation, and apoptosis(28, 29). JNKs form the last tier of the three-tier kinase module consisting of MAP kinase kinase kinase (MAP3K), MAP kinase kinase (MAP2K), and MAP kinase (MAPK)(28). Although early studies have identified JNK as an ultraviolet-responsive kinase, further studies have demonstrated a broader role for JNK in response to a variety of external stimuli such as cytokines, growth factors oxidative stress, and cytotoxic reagents(11, 28, 29, 46-48). The outcome of JNK activation, -whether it leads to cell proliferation or apoptosis, -depends on the cell type involved, the nature of the stimuli and the duration of JNK activation(28). Persistent JNK activation induced by DNA damage, oxidative stress, loss of matrix contact, deprivation of growth factors or chemotherapy treatment such as platinum leads to a robust pro-apoptotic response(11, 28, 29, 31, 46-48). Therefore, tight regulation of JNK activation is critical for maintaining cellular homeostasis and physiological functions.

Interestingly, it has been shown that the JNK pathway is activated differentially in response to cisplatin in ovarian cancer cells, with the cisplatin-sensitive cells showing prolonged activation (8–12 h) and the cisplatin-resistant cells showing only transient activation (1–3

h) of JNK(11), suggesting the duration of JNK activation is critical in determining whether cells survive or undergo apoptosis in response platinum treatment. Modulating platinum-induced JNK activation may be therapeutically exploited to enhance platinum efficacy; however, therapeutical manipulating JNK pathway to improve platinum efficacy remains unsuccessful due to the lack of comprehensive understanding of how JNK activation is regulated in response to platinum treatment. This study has identified SRMS an important negative regulator of MKK-JNK signaling under platinum treatment condition. Therapeutic targeting SRMS with small molecular inhibitor enhanced JNK activation and platinum efficacy *in vivo*, suggesting SRMS may represent a promising therapeutic target to boost platinum-based chemotherapy for ovarian cancer patients, especially for patients whose tumor shows elevated level of SRMS.

MATERIALS AND METHODS

Cell lines.

Human ovarian cancer cell lines including ES-2, OVCAR4, OVCAR3, OVCAR8, TOV21G and HEY were provided by Dr. Shuang Huang (University of Florida). Human ovarian cancer cell lines including CAOV3 and SKOV3 were purchased from American Type Culture Collection. KB-3-1 cells were obtained as previously described (49). KB-3-1 is a derivative of HeLa commonly used in multiple drug resistance studies (50). 293T cells were purchased from Takara Bio. All cell lines were authenticated by STR profiling. ES-2 cisplatin resistant and OVCAR4 carboplatin resistant sublines were generated using a dose escalating strategy, as previously described(14). Briefly, cells were initially treated with 0.5μg/ml of cisplatin (ES-2) or 5μg/ml of carboplatin (OVCAR4). After 48 hours, drug was removed, and fresh medium was added to the cells. After cells started growing again, another rounds of drug treatment with higher drug concentration were started (1μg/ml for cisplatin, and 10μg/ml carboplatin). Similar rounds of drug treatment with escalating dose were repeated until the cells can stand with 20μg/ml of cisplatin (ES-2) or 200μg/ml of carboplatin (OVCAR4).

Inhibitors and drugs.

Cisplatin, Carboplatin, Paclitaxel, JNK inhibitor II and Mitomycin C were purchased from Sigma-Aldrich. Etoposide, Camptothecin, Doxorubicin, Olaparib, SB203580, SCH772984, pLX4720, Dasatinib, Bosutinib, Foretinib, TAE684, PD173955, tamatinib, AST487, KI20227, and SU-14813 were purchased from Selleckchem.

Western blot and qRT-PCR.

Western blot and qRT-PCR were carried out according to previously established procedures(14, 51). The antibodies and Primers used in this study are listed in Tables S1-S2.

Lentivirus production and protein overexpression in human cancer cells.

To knock down endogenous human SRMS and MKK4, lentivirus carrying shRNA were generated by transfecting 293T cells with lentiviral vector encoding shRNA, psPAX2, and pMD2.G. The following shRNAs from TRC-Hs1.0 (Human) shRNA library were

used: shSRMS#1 (TRCN0000000938), shSRMS#4 (TRCN0000000941), and shMKK4#2 (TRCN0000001830).

Cell viability and caspase 3/7, 8, 9 activity assays.

Cell viability and Caspases activities were measured using CellTiter-Glo Luminescent Viability Assay and Caspase-Glo Assay System (Promega).

Colony formation assay.

For the colony forming assay, 300 ES-2 cells were seeded in 35-mm dishes and treated with PBS or cisplatin for 24 hours. The colonies were stained with 0.5% crystal violet after 7 days.

Flow cytometry analysis.

Flow cytometry analysis of γH2AX, cleaved-PARP, BrdU and 7-AAD was performed using Apoptosis, DNA Damage and Cell Proliferation Kit (BD) according to the manufacturer's instructions.

RNA-seq.

RNA was isolated by RNeasy kit (QIAGEN). RNA quantity check and sequencing was performed at UF ICBR Gene Expression and Genotyping Core (GE). The Gene Set Enrichment Analysis (GSEA) was accomplished by using the GSEA v4.1.0 software according to the instructions (http://www.broadinstitute.org/gsea/index.jsp).

Phospho-kinase array.

Phospho-kinase array was performed using Proteome Profiler Human Phospho-Kinase Array (R&D, ARY003B) according to manufacturer's instructions.

Bimolecular fluorescence complementation (BiFC) assay and comet assay.

The vectors pDEST-ORF-V1 (Addgene #73637) and pDEST-ORF-V2 (Addgene #73638) were gifts from Darren Saunders(33). The pENTR223.1-SRMS (DNASU #HscD00350795) or pDONR223_MAP2K4 (a gift from Jesse Boehm & William Hahn & David Root, Addgene #82142) was cloned into pDEST-V1 or pDEST-V2 destination vectors. The BiFC assay was conducted as previous described(33). Comet assay was conducted as previously deprescribed(52).

In vitro kinase assays and mass spectrometry.

ES-2 overexpressing FLAG-tagged human SRMS was established and FLAG-SRMS was immunoprecipitated by ANTI-FLAG M2 Affinity Gel (Millipore A2220), followed by a kinase assay (40 mM Tris [pH 7.5], 20 mM MgCl2, 2mM MnCl2, 50uM DTT, and 200 mM ATP). For mass spectrometry, FLAG-SRMS was immunoprecipitated and a kinase assay was performed using recombinant GST-MKK4 (Abnova) as a substrate. A gel piece corresponding to GST-MKK4 was analyzed by mass spectrometry (MS Bioworks LLC, MI).

MCL1 promoter activity assay and CUT & RUN.

The promoter pGL2-Mcl-1 was a gift from Wafik El-Deiry (Addgene plasmid # 19132)(53). The pGL2-Empty control-SV40-Luc was a gift from Rudolf Jaenisch (Addgene plasmid # 26280)(54). Cleavage Under Targets & Release Using Nuclease (CUT&RUN) was performed using CUT&RUN Assay (Cell Signaling Technology). The quantification was done by qPCR. Primer for MCL-1 promoter was F: 5'-TAGGACTGGCCGCCCTAAAA-3', R: 5'-CCCCCCACAGTAGAGGTTGA-3'.

Xenograft studies.

Animal studies were performed according to protocols reviewed and approved by the Institutional Animal Care and Use Committee of University of Florida and University of Texas Health Science Center at San Antonio. Female nude mice at 4–6-weeks old were purchased from the Jackson Laboratory. 5×10^5 ES-2-BLI cell were intravenously injected into the mice at Day 0. For the SRMS knockdown experiment, vehicle control or cisplatin was given starting from Day 3 at 10 mg/kg at the first week. For the pLX4720 efficacy experiment, vehicle control or pLX4720 was started on Day 3 at 25 mg/kg, daily; cisplatin administration was started on Day 7 at 2.5 mg/kg per week for ES-2 parental cells and 5mg/kg for cisplatin resistant cells. Tumor growth was monitored by bioluminescence imaging (BLI) as previously described(51, 55).

Immunohistochemical staining.

The paraffin-embedded high-density ovarian carcinoma tissue microarray (OV2001b) was purchased from US Biomax. IHC analyses were performed as previously described(14).

Quantification and statistical analysis.

Statistical parameters including the statistical tests used, exact value of n, and statistical significance are reported in the figures and figure legends. Each dot represents one experimental result. Data with error bars represent mean ± SD. No statistical method was used to predetermine sample size. Statistical analysis of significance was based on two-tailed Student's t test unless specified in figure legends. For all animal studies, animals were randomly chosen. Concealed allocation and blinding of outcome assessment were used. Statistical tests performed are based on a set of assumptions including normal distribution and homogeneity of variances. The variability within each group has been quantified with standard deviation and used for statistical comparison.

Publicly available TCGA database analysis.

Protein kinase mRNA expression z-scores and cisplatin/carboplatin sensitivity data were downloaded from Depmap portal.

Supplementary Material

Refer to Web version on PubMed Central for supplementary material.

ACKNOWLEDGEMENTS

We acknowledge Ryan Clay for editorial assistance.

Funding:

This work was supported in part by NIH grants R37 CA249305 (L.J.), R01CA269782 (L.J.), R01 CA256482 (S.H. and L.J.), DoD LCRP Career Development Award W81XWH2010309 (L.J.), Lung Cancer Research Foundation pilot grant (L.J.) and American Lung Association Innovation Award (L.J.).

DATA AVAILABILITY

All data needed to evaluate the conclusions in the paper are present in the paper and/or the Supplementary Materials. RNA sequencing data has been deposited to GEO repository (GSE206226). Additional data related to this paper may be requested from the authors.

REFERENCES

1. Jayson GC, Kohn EC, Kitchener HC, and Ledermann JA. Ovarian cancer. Lancet. 2014;384(9951):1376–88. [PubMed: 24767708]
2. Barber E, and Matei D. Immunotherapy in ovarian cancer: we are not there yet. Lancet Oncol. 2021;22(7):903–5. [PubMed: 34143972]
3. Chardin L, and Leary A. Immunotherapy in Ovarian Cancer: Thinking Beyond PD-1/PD-L1. Front Oncol. 2021;11:795547. [PubMed: 34966689]
4. Pujade-Lauraine E, Fujiwara K, Ledermann JA, Oza AM, Kristeleit R, Ray-Coquard IL, et al. Avelumab alone or in combination with chemotherapy versus chemotherapy alone in platinum-resistant or platinum-refractory ovarian cancer (JAVELIN Ovarian 200): an open-label, three-arm, randomised, phase 3 study. Lancet Oncol. 2021;22(7):1034–46. [PubMed: 34143970]
5. Matulonis UA, Sood AK, Fallowfield L, Howitt BE, Sehouli J, and Karlan BY. Ovarian cancer. Nat Rev Dis Primers. 2016;2:16061. [PubMed: 27558151]
6. Siddik ZH. Cisplatin: mode of cytotoxic action and molecular basis of resistance. Oncogene. 2003;22(47):7265–79. [PubMed: 14576837]
7. Murata T, Haisa M, Uetsuka H, Nobuhisa T, Ookawa T, Tabuchi Y, et al. Molecular mechanism of chemoresistance to cisplatin in ovarian cancer cell lines. International journal of molecular medicine. 2004;13(6):865–8. [PubMed: 15138626]
8. Galluzzi L, Senovilla L, Vitale I, Michels J, Martins I, Kepp O, et al. Molecular mechanisms of cisplatin resistance. Oncogene. 2012;31(15):1869–83. [PubMed: 21892204]
9. Rottenberg S, Disler C, and Perego P. The rediscovery of platinum-based cancer therapy. Nat Rev Cancer. 2021;21(1):37–50. [PubMed: 33128031]
10. Brozovic A, and Osmak M. Activation of mitogen-activated protein kinases by cisplatin and their role in cisplatin-resistance. Cancer letters. 2007;251(1):1–16. [PubMed: 17125914]
11. Mansouri A, Ridgway LD, Korapati AL, Zhang Q, Tian L, Wang Y, et al. Sustained activation of JNK/p38 MAPK pathways in response to cisplatin leads to Fas ligand induction and cell death in ovarian carcinoma cells. The Journal of biological chemistry. 2003;278(21):19245–56. [PubMed: 12637505]
12. Persons DL, Yazlovitskaya EM, and Pelling JC. Effect of extracellular signal-regulated kinase on p53 accumulation in response to cisplatin. The Journal of biological chemistry. 2000;275(46):35778–85. [PubMed: 10958792]
13. Wang X, Martindale JL, and Holbrook NJ. Requirement for ERK activation in cisplatin-induced apoptosis. The Journal of biological chemistry. 2000;275(50):39435–43. [PubMed: 10993883]
14. Jin L, Chun J, Pan C, Li D, Lin R, Alesi GN, et al. MAST1 Drives Cisplatin Resistance in Human Cancers by Rewiring cRaf-Independent MEK Activation. Cancer Cell. 2018;34(2):315–30 e7. [PubMed: 30033091]

15. Park JM, Yang SW, Zhuang W, Bera AK, Liu Y, Gurbani D, et al. The nonreceptor tyrosine kinase SRMS inhibits autophagy and promotes tumor growth by phosphorylating the scaffolding protein FKBP51. PLoS Biol. 2021;19(6):e3001281. [PubMed: 34077419]
16. Ghandi M, Huang FW, Jane-Valbuena J, Kryukov GV, Lo CC, McDonald ER 3rd, et al. Next-generation characterization of the Cancer Cell Line Encyclopedia. Nature. 2019;569(7757):503–8. [PubMed: 31068700]
17. Iorio F, Knijnenburg TA, Vis DJ, Bignell GR, Menden MP, Schubert M, et al. A Landscape of Pharmacogenomic Interactions in Cancer. Cell. 2016;166(3):740–54. [PubMed: 27397505]
18. Prislei S, Mariani M, Raspaglio G, Mozzetti S, Filippetti F, Ferrandina G, et al. RON and cisplatin resistance in ovarian cancer cell lines. Oncol Res. 2010;19(1):13–22. [PubMed: 21141737]
19. Lanczky A, and Gyorffy B. Web-Based Survival Analysis Tool Tailored for Medical Research (KMplot): Development and Implementation. J Med Internet Res. 2021;23(7):e27633. [PubMed: 34309564]
20. Labidi-Galy SI, Papp E, Hallberg D, Niknafs N, Adleff V, Noe M, et al. High grade serous ovarian carcinomas originate in the fallopian tube. Nat Commun. 2017;8(1):1093. [PubMed: 29061967]
21. Ishikawa T, and Ali-Osman F. Glutathione-associated cis-diamminedichloroplatinum(II) metabolism and ATP-dependent efflux from leukemia cells. Molecular characterization of glutathione-platinum complex and its biological significance. J Biol Chem. 1993;268(27):20116–25. [PubMed: 8376370]
22. Wang W, Kryczek I, Dostal L, Lin H, Tan L, Zhao L, et al. Effector T Cells Abrogate Stroma-Mediated Chemoresistance in Ovarian Cancer. Cell. 2016;165(5):1092–105. [PubMed: 27133165]
23. Shen DW, Pouliot LM, Hall MD, and Gottesman MM. Cisplatin resistance: a cellular self-defense mechanism resulting from multiple epigenetic and genetic changes. Pharmacol Rev. 2012;64(3):706–21. [PubMed: 22659329]
24. De Luca A, Parker LJ, Ang WH, Rodolfo C, Gabbarini V, Hancock NC, et al. A structure-based mechanism of cisplatin resistance mediated by glutathione transferase P1-1. Proc Natl Acad Sci U S A. 2019;116(28):13943–51. [PubMed: 31221747]
25. Giannoni E, Buricchi F, Raugei G, Ramponi G, and Chiarugi P. Intracellular reactive oxygen species activate Src tyrosine kinase during cell adhesion and anchorage-dependent cell growth. Mol Cell Biol. 2005;25(15):6391–403. [PubMed: 16024778]
26. Meurer S, Pioch S, Gross S, and Muller-Esterl W. Reactive oxygen species induce tyrosine phosphorylation of and Src kinase recruitment to NO-sensitive guanylyl cyclase. J Biol Chem. 2005;280(39):33149–56. [PubMed: 16079134]
27. Li J, Zheng C, Wang M, Umano AD, Dai Q, Zhang C, et al. ROS-regulated phosphorylation of ITPKB by CAMK2G drives cisplatin resistance in ovarian cancer. Oncogene. 2022;41(8):1114–28. [PubMed: 35039634]
28. Dhanasekaran DN, and Reddy EP. JNK signaling in apoptosis. Oncogene. 2008;27(48):6245–51. [PubMed: 18931691]
29. Girnius N, and Davis RJ. JNK Promotes Epithelial Cell Anoikis by Transcriptional and Post-translational Regulation of BH3-Only Proteins. Cell Rep. 2017;21(7):1910–21. [PubMed: 29141222]
30. Girnius N, Edwards YJ, Garlick DS, and Davis RJ. The cJUN NH2-terminal kinase (JNK) signaling pathway promotes genome stability and prevents tumor initiation. Elife. 2018;7.
31. Miura H, Kondo Y, Matsuda M, and Aoki K. Cell-to-Cell Heterogeneity in p38-Mediated Cross-Inhibition of JNK Causes Stochastic Cell Death. Cell Rep. 2018;24(10):2658–68. [PubMed: 30184500]
32. Zeke A, Misheva M, Remenyi A, and Bogoyevitch MA. JNK Signaling: Regulation and Functions Based on Complex Protein-Protein Partnerships. Microbiol Mol Biol Rev. 2016;80(3):793–835. [PubMed: 27466283]
33. Croucher DR, Iconomou M, Hastings JF, Kennedy SP, Han JZ, Shearer RF, et al. Bimolecular complementation affinity purification (BiCAP) reveals dimer-specific protein interactions for ERBB2 dimers. Sci Signal. 2016;9(436):ra69. [PubMed: 27405979]

34. Wang W, Wang YQ, Meng T, Yi JM, Huan XJ, Ma LP, et al. MCL-1 degradation mediated by JNK activation via MEKK1/TAK1-MKK4 contributes to anticancer activity of new tubulin inhibitor MT189. Mol Cancer Ther. 2014;13(6):1480–91. [PubMed: 24688049]
35. Ding Q, He X, Hsu JM, Xia W, Chen CT, Li LY, et al. Degradation of Mcl-1 by beta-TrCP mediates glycogen synthase kinase 3-induced tumor suppression and chemosensitization. Mol Cell Biol. 2007;27(11):4006–17. [PubMed: 17387146]
36. Morel C, Carlson SM, White FM, and Davis RJ. Mcl-1 integrates the opposing actions of signaling pathways that mediate survival and apoptosis. Mol Cell Biol. 2009;29(14):3845–52. [PubMed: 19433446]
37. Thomas LW, Lam C, and Edwards SW. Mcl-1; the molecular regulation of protein function. FEBS Lett. 2010;584(14):2981–9. [PubMed: 20540941]
38. Skene PJ, Henikoff JG, and Henikoff S. Targeted in situ genome-wide profiling with high efficiency for low cell numbers. Nat Protoc. 2018;13(5):1006–19. [PubMed: 29651053]
39. Skene PJ, and Henikoff S. An efficient targeted nuclease strategy for high-resolution mapping of DNA binding sites. Elife. 2017;6.
40. Davis MI, Hunt JP, Herrgard S, Ciceri P, Wodicka LM, Pallares G, et al. Comprehensive analysis of kinase inhibitor selectivity. Nat Biotechnol. 2011;29(11):1046–51. [PubMed: 22037378]
41. Tsai J, Lee JT, Wang W, Zhang J, Cho H, Mamo S, et al. Discovery of a selective inhibitor of oncogenic B-Raf kinase with potent antimelanoma activity. Proc Natl Acad Sci U S A. 2008;105(8):3041–6. [PubMed: 18287029]
42. Vin H, Ojeda SS, Ching G, Leung ML, Chitsazzadeh V, Dwyer DW, et al. BRAF inhibitors suppress apoptosis through off-target inhibition of JNK signaling. Elife. 2013;2:e00969. [PubMed: 24192036]
43. Wenglowsky S, Ahrendt KA, Buckmelter AJ, Feng B, Gloor SL, Gradl S, et al. Pyrazolopyridine inhibitors of B-RafV600E. Part 2: structure-activity relationships. Bioorg Med Chem Lett. 2011;21(18):5533–7. [PubMed: 21802293]
44. Goel RK, Miah S, Black K, Kalra N, Dai C, and Lukong KE. The unique N-terminal region of SRMS regulates enzymatic activity and phosphorylation of its novel substrate docking protein 1. FEBS J. 2013;280(18):4539–59. [PubMed: 23822091]
45. Goel RK, Paczkowska M, Reimand J, Napper S, and Lukong KE. Phosphoproteomics Analysis Identifies Novel Candidate Substrates of the Nonreceptor Tyrosine Kinase, Src-related Kinase Lacking C-terminal Regulatory Tyrosine and N-terminal Myristoylation Sites (SRMS). Mol Cell Proteomics. 2018;17(5):925–47. [PubMed: 29496907]
46. Cano E, Hazzalin CA, and Mahadevan LC. Anisomycin-activated protein kinases p45 and p55 but not mitogen-activated protein kinases ERK-1 and -2 are implicated in the induction of c-fos and c-jun. Mol Cell Biol. 1994;14(11):7352–62. [PubMed: 7935449]
47. Sluss HK, Barrett T, Derijard B, and Davis RJ. Signal transduction by tumor necrosis factor mediated by JNK protein kinases. Mol Cell Biol. 1994;14(12):8376–84. [PubMed: 7969172]
48. Westwick JK, Weitzel C, Minden A, Karin M, and Brenner DA. Tumor necrosis factor alpha stimulates AP-1 activity through prolonged activation of the c-Jun kinase. J Biol Chem. 1994;269(42):26396–401. [PubMed: 7929360]
49. Richert N, Akiyama S, Shen D, Gottesman MM, and Pastan I. Multiply drug-resistant human KB carcinoma cells have decreased amounts of a 75-kDa and a 72-kDa glycoprotein. Proceedings of the National Academy of Sciences of the United States of America. 1985;82(8):2330–3. [PubMed: 3857583]
50. Hall MD, Telma KA, Chang KE, Lee TD, Madigan JP, Lloyd JR, et al. Say no to DMSO: dimethylsulfoxide inactivates cisplatin, carboplatin, and other platinum complexes. Cancer research. 2014;74(14):3913–22. [PubMed: 24812268]
51. Jin L, Chun J, Pan C, Kumar A, Zhang G, Ha Y, et al. The PLAG1-GDH1 Axis Promotes Anoikis Resistance and Tumor Metastasis through CamKK2-AMPK Signaling in LKB1-Deficient Lung Cancer. Mol Cell. 2018;69(1):87–99 e7. [PubMed: 29249655]
52. Olive PL, and Banath JP. The comet assay: a method to measure DNA damage in individual cells. Nat Protoc. 2006;1(1):23–9. [PubMed: 17406208]

53. Ricci MS, Kim SH, Ogi K, Plastaras JP, Ling J, Wang W, et al. Reduction of TRAIL-induced Mcl-1 and cIAP2 by c-Myc or sorafenib sensitizes resistant human cancer cells to TRAIL-induced death. Cancer Cell. 2007;12(1):66–80. [PubMed: 17613437]

54. Hanna J, Cheng AW, Saha K, Kim J, Lengner CJ, Soldner F, et al. Human embryonic stem cells with biological and epigenetic characteristics similar to those of mouse ESCs. Proc Natl Acad Sci U S A. 2010;107(20):9222–7. [PubMed: 20442331]

55. Alesi GN, Jin L, Li D, Magliocca KR, Kang Y, Chen ZG, et al. RSK2 signals through stathmin to promote microtubule dynamics and tumor metastasis. Oncogene. 2016;35(41):5412–21. [PubMed: 27041561]

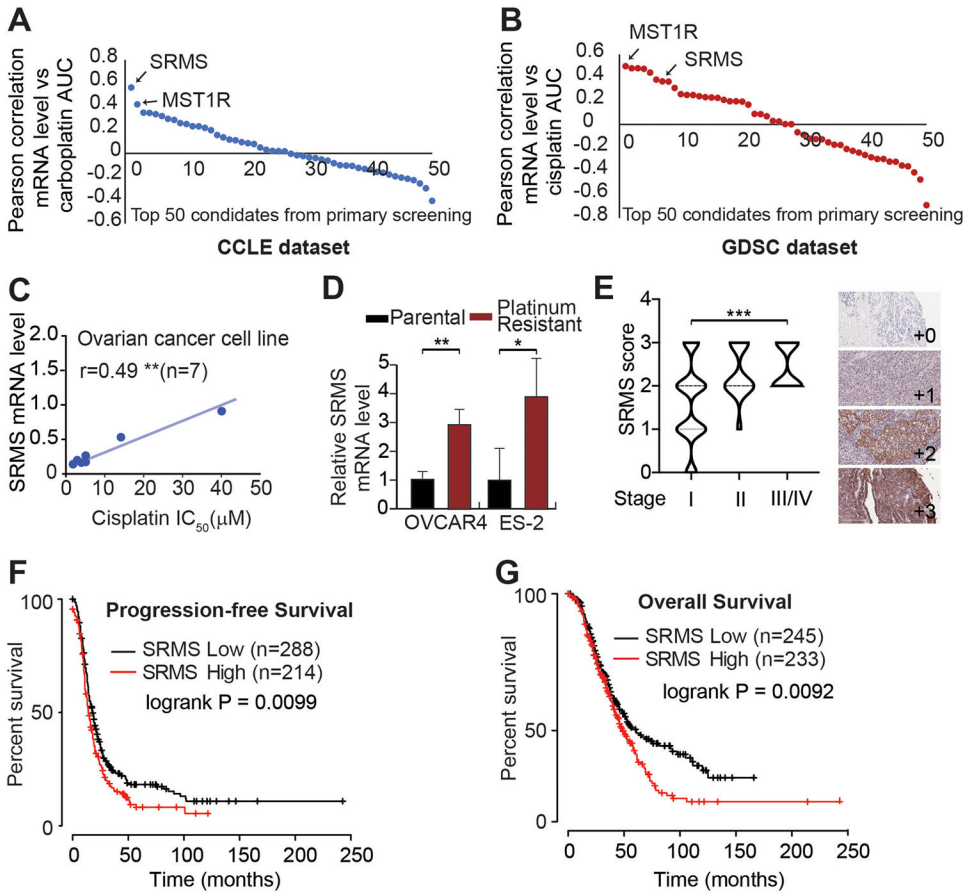

Figure 1. Identification of SRMS as a potential driver of platinum resistance in human ovarian cancer.

(A-B) Pearson correlation analysis between SRMS level (RNAseq) and carboplatin/cisplatin sensitivity (AUC) using Cancer Cell Line Encyclopedia database (CCLE) and Sanger Genomics of Drug Sensitivity in Cancer database (GDSC). **(C)** Pearson correlation between cisplatin IC_{50} (cell viability assay, 72 hours) and SRMS mRNA levels (qRT-PCR) of ovarian cancer cell lines. **(D)** qRT-PCR analysis of SRMS mRNA levels in ovarian cancer parental and platinum resistant sublines. **(E)** Immunohistochemical staining using primary tissue microarray samples from ovarian cancer patients. **(F-G)** Overall survival (F) and progression free survival (G) of platinum-treated ovarian cancer patients. Kaplan–Meier graph is shown. Data are mean ± SD from three independent technical replicates and are representative of three independent biological experiments for (C-D). Statistical analyses were performed by Pearson's correlation coefficient for (A-C), unpaired 2-tailed *t* test for (D), 1-way ANOVA for (E), and logrank test for (F-G). (ns: not significant; **P*<0.05; ***P*<0.01; ****P*<0.001).

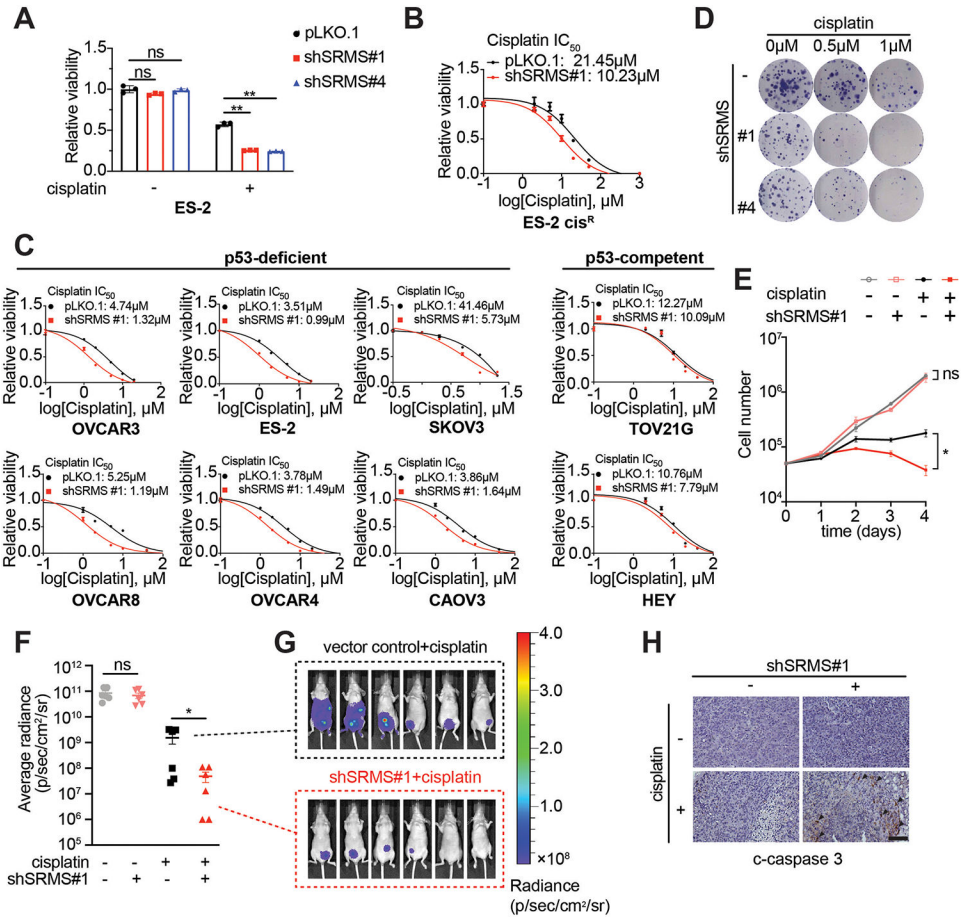

Figure 2. Silencing SRMS sensitizes cisplatin treatment *in vitro* and *in vivo*.

(A) Cell viability of ovarian cancer ES-2 cell with or without SRMS shRNA. Cells expressing two different SRMS shRNA clones or control vector were treated with cisplatin (1.875uM) or vehicle control. Cell viability was assessed by CellTiter-Glo viability assay after 72 hours of treatment. **(B)** ES-2 cisplatin-resistant cells expressing SRMS shRNA#1 or control vector were treated with cisplatin or vehicle for 72 hours. Cisplatin IC_{50} was assessed using CellTiter-Glo viability assay. **(C)** Multiple ovarian cancer cells with or without SRMS knockdown were treated with different concentrations of cisplatin for 72 hours. Cell viability was determined by CellTiter-Glo Luminescent Viability assay. **(D)** Colony-formation assays (7days) were performed using ES-2 cells with or without SRMS knockdown and cisplatin treatment. **(E)** ES-2 cells with or without SRMS knockdown were treated with cisplatin, and cell counting was performed at indicated time points. **(F-H)** Effect of cisplatin treatment and SRMS knockdown on tumor growth of ES-2 xenograft mice. Nude mice were injected with ES-2-GFP-luciferase cells with or without SRMS knockdown and treated with cisplatin or vehicle control (5mg/kg). Average photonic flux (F), bioluminescence images (G), and representative images of cleaved caspase-3 immunohistochemical (IHC) staining in harvested tumors (H) from each group at day 24 post tumor injection are shown. Scale bars represent 100 mm. Data are mean ± SD from three independent technical replicates for (A-C, E) and are representative of three

independent biological experiments for (A-E). Statistical analyses were performed by unpaired 2-tailed t test for (A, E, F). (ns: not significant; *P<0.05; **P<0.01).

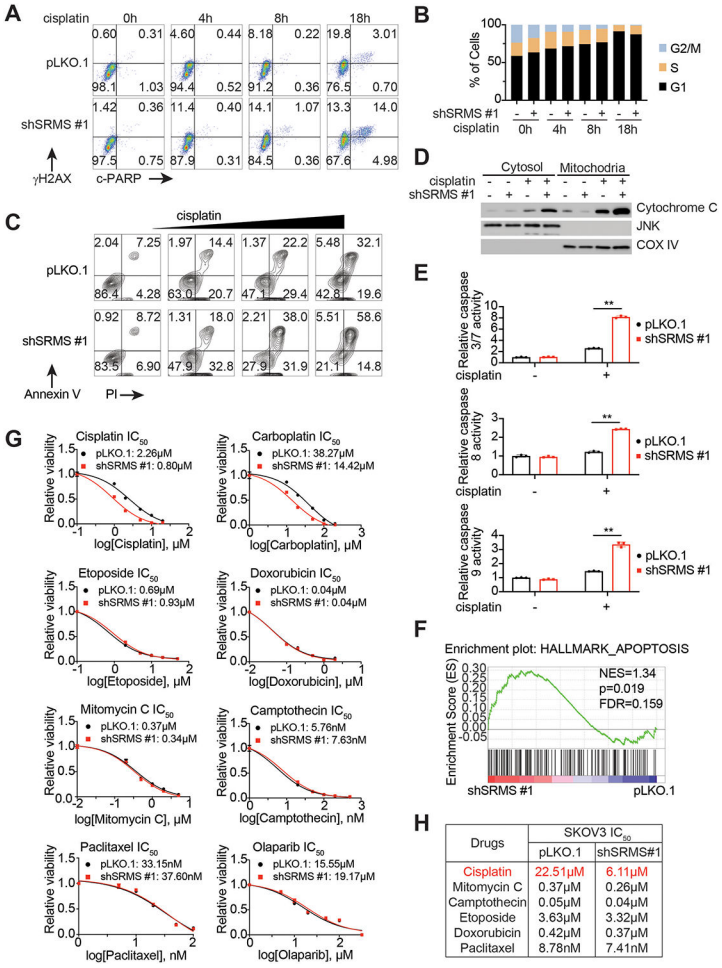

Drugs	SKOV3 IC_{50}	
	pLKO.1	shSRMS#1
Cisplatin	22.51μM	6.11μM
Mitomycin C	0.37μM	0.26μM
Camptothecin	0.05μM	0.04μM
Etoposide	3.63μM	3.32μM
Doxorubicin	0.42μM	0.37μM
Paclitaxel	8.78nM	7.41nM

Figure 3. SRMS silencing promotes platinum-induced apoptosis.

(A-B) Flow cytometric analysis of DNA damage, cell apoptosis and cell cycle distribution. ES-2 cells were treated with 15μM cisplatin and collected at indicated time points for flow cytometric analysis of DNA damage (A, γH2AX), apoptosis (A, cleaved-PARP), and cell cycle distribution (B, 7-AAD). **(C)** Apoptosis assay with Annexin V/PI staining in ES-2 cells expressing control vector or SRMS shRNA treated with different concentrations of cisplatin (from left to right: 0μM, 2.5μM, 5μM, 7.5μM) for 48 hours. **(D)** ES-2 cells expressing control vector or SRMS shRNA were treated with 15μM cisplatin for 25 hours, followed by cytosol and mitochondria fractionation and western blotting analysis of cytochrome c. **(E)** ES-2 cells expressing control vector or SRMS shRNA were treated with or without 15μM cisplatin for 24 hours and activities of caspase 3/7 (top), caspase 8 (middle), caspase 9 (bottom) were determined by Caspase-Glo 3/7, Caspase-Glo 8, Caspase-Glo 9 activity assay, respectively. **(F)** RNA-seq analysis of ES-2 cells expressing control vector or SRMS shRNA were treated with 15μM cisplatin for 8 hours. Gene set enrichment analysis (GSEA) plot of apoptosis from hallmark categories of SRMS knockdown versus control are shown. **(G-H)** ES-2 (G) and SKOV3 (H) cells with or without SRMS knockdown were treated with different concentrations of DNA damaging agents or cytotoxic drugs for 72 hours. Cell viability and IC_{50} was determined by CellTiter-Glo assay. Data are mean ±

SD from three independent technical replicates for (E and G) and are representative of three independent biological experiments for (A-E, G-H). Statistical analyses were performed by unpaired 2-tailed t test for (E). (ns: not significant; *P<0.05; **P<0.01).

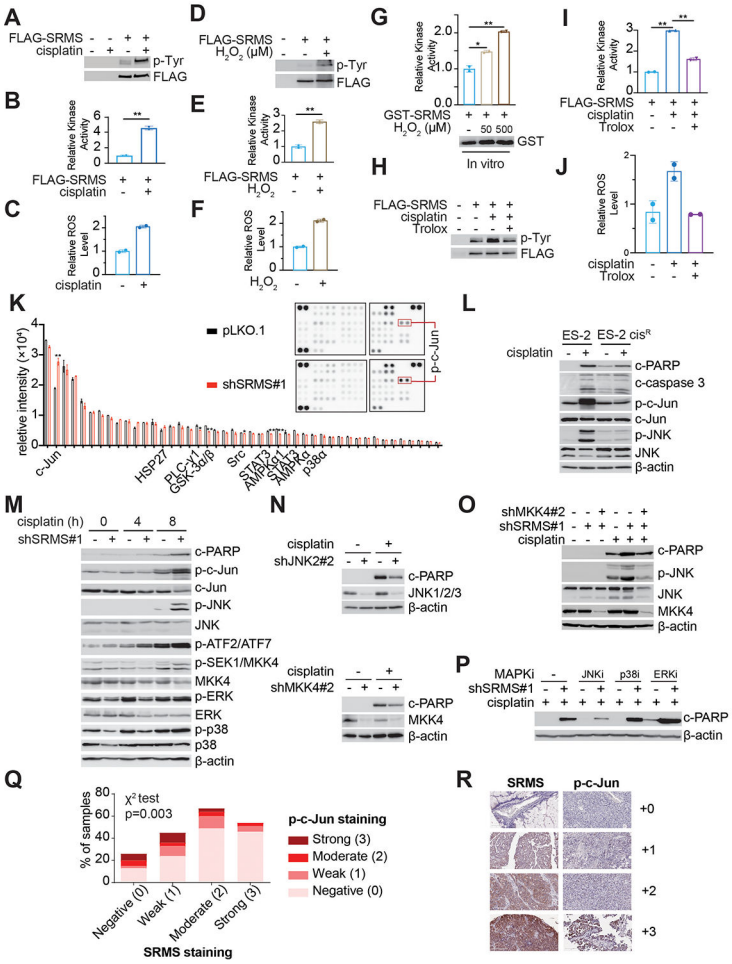

Figure 4. Silencing SRMS leads to hyper-activation of MKK4-JNK-c-Jun axis upon platinum treatment.

(A-F) ES-2 cells were treated with 20μM cisplatin (A-C) or 100μM H_2O_2 (D-F) for 16 hours, followed by FLAG-immunoprecipitation. SRMS autophosphorylation (A and D), kinase activity (B and E) and ROS levels were determined using western blotting, ADP-glo kinase assay, H_2DCFDA staining, respectively. **(G)** 293T cell was transfected with GST-SRMS followed by GST-immunoprecipitated. GST-SRMS were incubated with H_2O_2 *in vitro* in kinase reaction buffer and kinase activity was determined by ADP-glo kinase assay. **(H-J)** ES-2 cells were treated with 20μM cisplatin with or without 1mM antioxidant Trolox for 16 hours, followed by FLAG-immunoprecipitation. SRMS autophosphorylation (H), kinase activity (I) and ROS levels were determined. **(K)** Phospho-kinase proteome profiling of ES-2 cells with or without SRMS knockdown and cisplatin treatment (15μM for 8 hours). Relative intensity was determined. **(L)** ES-2 parental and cisplatin-resistant subline were treated with vehicle control or cisplatin (15μM for 16 hours), followed by western blotting analysis. **(M)** ES-2 cells expressing control vector or SRMS shRNA were treated with 15μM cisplatin, followed by western blotting at indicated time points. **(N)** ES-2 cells expressing control vector or JNK2 shRNA (top) or MKK4 shRNA (bottom) were treated with vehicle control or cisplatin (15μM for 16 hours), followed by western blotting analysis. **(O)** ES-2 cells expressing SRMS and MKK4 shRNA were treated with 15μM cisplatin for 16 hours.

Cell apoptosis and JNK activation were determined by western blotting of cleaved-PARP and p-JNK. **(P)** ES-2 cells expressing control vector or SRMS shRNA were treated with cisplatin (15μM, 16 hours) in the presence or absence of JNK inhibitor II (JNKi, 20μM), SB203580 (p38i, 10μM) and SCK772984 (ERKi, 2μM). Cell apoptosis was determined by western blotting of cleaved PARP (c-PARP). **(Q)** The correlation between levels of SRMS and activated c-Jun (phospho-c-Jun S73) determined by immunohistochemistry in ovarian cancer patient samples. **(R)** Representative IHC images for SRMS and phospho-c-Jun are presented on the right for 0, +1, and +2 scores. Scale bars represent 100 mm. p value was determined by chi-square test. Data are mean ± SD from two independent technical replicates for (B,C,E,F,G,I,J) and are representative of three independent biological experiments for (A-J,L-P). (ns: not significant; *P<0.05; **P<0.01).

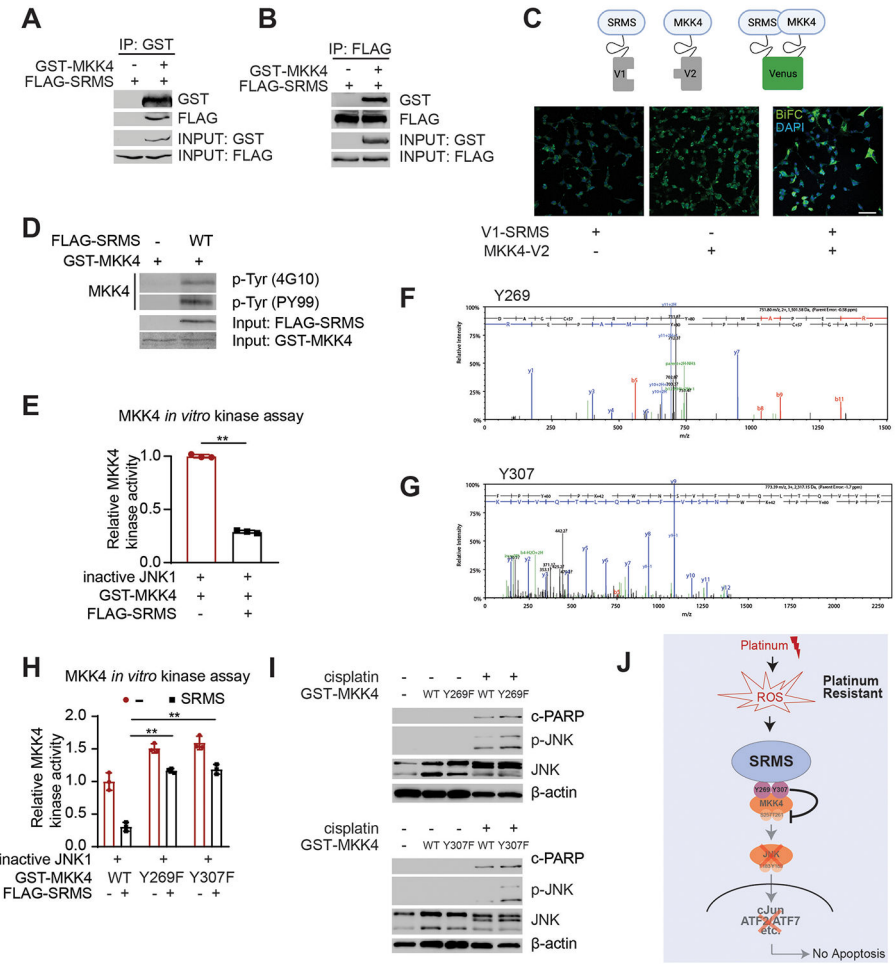

Figure 5. SRMS directly phosphorylates MKK4 and inhibits MKK4-JNK-c-Jun activation upon platinum treatment.

(A-B) Direct binding between SRMS and MKK4. 293T cells were transfected with GST-MKK4 and FLAG-SRMS for 24 hours, followed by immunoprecipitation and immunoblotting. **(C)** Interaction between SRMS and MKK4 was assessed by Bimolecular Fluorescence Complementation (BiFC) assay in ES-2 cells. Scale bar, 100μm. **(D)** *In vitro* SRMS kinase assay. FLAG-SRMS was immunoprecipitated from ES-2 cells, followed by *in vitro* kinase assay using GST-MKK4 as substrate. MKK4 tyrosine phosphorylation was determined by immunoblotting using two different phospho-tyrosine antibody, clone 4G10 and PY99. **(E)** Two-stage SRMS-MKK4 *in vitro* kinase assay. GST-MKK4 was incubated with or without FLAG-SRMS for SRMS *in vitro* kinase assay. Then GST-MKK4 were recovered by GST pulldown, extensively washed and subjected to MKK4 *in vitro* kinase assay using inactive JNK1 as substrate. MKK4 activity was determined by ADP-Glo assay. **(F-G)** Identification of tyrosine phosphorylation sites in MKK4 protein. GST-MKK4 was phosphorylated by SRMS using *in vitro* kinase assay and subjected to mass spectrometry analysis. The tandem mass spectrum of the peptides contains c-Y269 (E) and phospho-Y307 (F) are shown. **(H)** Effect of phospho-deficient mutant (Y269F or Y307F) on MKK4 kinase activity. Two stage SRMS MKK4 *in vitro* kinase assay with or without SRMS using MKK4 WT, MKK4 Y269F or MKK4 Y307F mutant was performed as in (E). MKK4 activity

was determined by ADP-Glo assay. **(I)** Effect of phospho-deficient mutant MKK4 (Y269F, top or Y307F, bottom) on cisplatin-induced JNK activation in ES-2 cells. **(J)** Proposed model for SRMS-medicated inhibition of MKK4-JNK signaling in ovarian cancer. Data are representative of three independent biological experiments for (A-E, H-I).

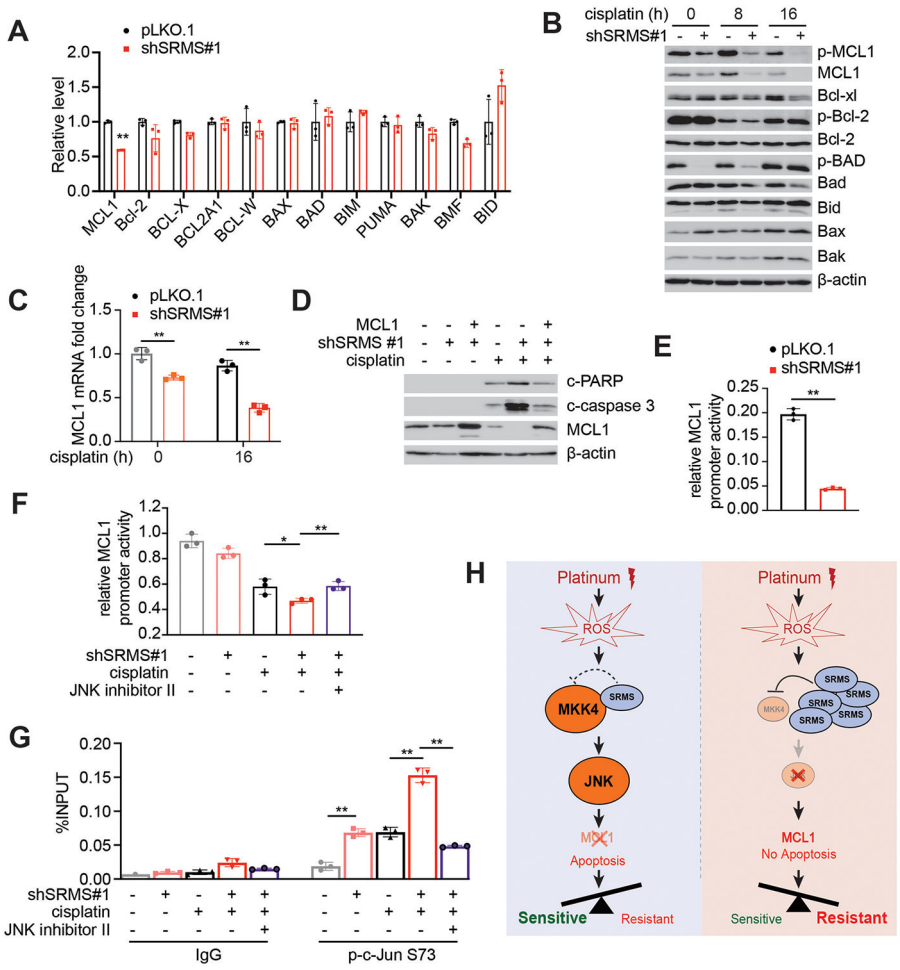

Figure 6. SRMS sustains MCL-1 gene transcription to confer platinum resistance.

(A-B) qRT-PCR (A) and western blotting (B) analysis of gene expression of Bcl-2 family members in ES-2 cells expressing control vector or SRMS shRNA upon 15μM cisplatin treatment (8 hours for qRT-PCR). **(C)** ES-2 cells expressing control vector or SRMS shRNA were treated with cisplatin (15μM) for indicated time points, and MCL1 mRNA levels were determined by qRT-PCR. **(D)** Ectopic MCL1 expression rescues enhanced apoptosis in SRMS knockdown cells with cisplatin treatment. **(E)** MCL1 promoter activity was determined in control or SRMS knockdown ES-2 cells that were treated with 15μM cisplatin for 16 hours. **(F)** JNK inhibitor II treatment rescues reduced MCL-1 promoter activity in SRMS knockdown cells with cisplatin treatment. ES-2 cells expressing control vector or SRMS shRNA were treated with cisplatin and JNK inhibitor for 6h, followed by MCL1 promoter activity assay. **(G)** p-c-Jun (S73) CUT&RUN and qPCR on MCL-1 promoter region. ES-2 cells expressing control vector or SRMS shRNA were treated with cisplatin and JNK inhibitor II for 6h. **(H)** Proposed model for the role of SRMS in cisplatin resistance in human cancer. Data are mean ± SD from three independent technical replicates for (A,C,E-G) and are representative of three independent biological experiments for (A-G).

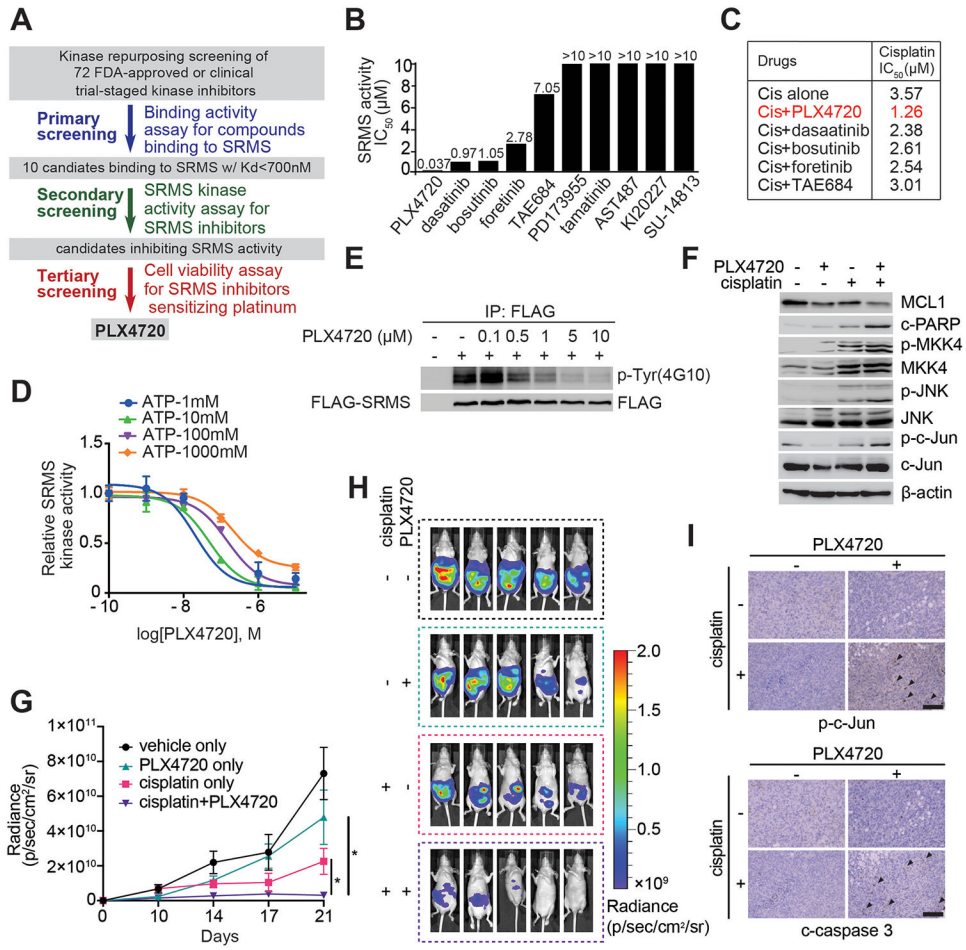

Figure 7. Characterization of pLX4720 as a potential SRMS inhibitor that can boost platinum efficacy in ovarian cancer cells *in vitro* and *in vivo*.

(A) Screening strategy to identify potential SRMS inhibitors. **(B)** Top ten candidates that potentially bind to SRMS were evaluated for their inhibitor activity using *in vitro* SRMS kinase assay. Compounds (10 μM) were incubated with purified FLAG-SRMS and applied to the SRMS *in vitro* kinase assay. **(C)** Top five SRMS inhibitors from (B) were evaluated for their cisplatin sensitizing activity in ES-2 cells using Cell-Titer Glo assay. Cisplatin IC_{50} are shown. **(D)** Effect of PLX4720 on SRMS kinase activity using ADP-Glo kinase activity assay at a range of ATP concentrations. **(E)** Effect of pLX4720 on SRMS autophosphorylation determined by immunoblotting with phospho-tyrosine antibody clone 4G10. **(F)** Effect of PLX4720 on JNK signaling and platinum-induced apoptosis. **(G-I)** Effect of cisplatin and pLX4720 treatment on tumor growth of ES-2 xenograft mice. Nude mice were injected with ES-2-GFP-luciferase cells and average photonic flux and bioluminescence images of each group at day 24 post-tumor injection are shown (G and H). Representative images of p-c-Jun and cleaved caspase-3 analyzed by immunohistochemical (IHC) staining in harvested tumors from each group (I) . Scale bars represent 100 mm. Data are mean ± SD from three independent technical replicates for (D) and mean ± SEM from 5

mice for (G). Data are representative of three independent biological experiments for (D-E). P values were determined by two-tailed Student's t test (ns, not significant; *p < 0.05).